J Nondestruct Eval (2010) 29: 169–174
DOI 10.1007/s10921-010-0074-4

Automatic Crack Detection and Characterization During Ultrasonic Inspection

Thouraya Merazi Meksen · Bachir Boudraa · Redouane Drai · Malika Boudraa

Published online: 23 June 2010

Abstract The creation of a non-destructive technique that enables the automatic detection of defects is desirable, and TOFD (Time-Of-Flight Diffraction) technique is gaining rapid prominence due to its high accuracy in detecting, positioning and sizing flaws in steel structures. In this type of imaging, cracks are characterized using sets of hyperbolas, where summit positions correspond to crack tip positions. However, ultrasonic diffracted signals are often too low and difficult to distinguish from noise, and when large structures are inspected, the quantity of data can be extremely large, with the area of interest being very small in comparison to the image size. This paper describes a method that avoids the image formation, replacing it with a sparse matrix (as there is no reason to store and operate on an excessive number of zeros), and automates crack detection by analyzing the curve formed by the sparse matrix elements. The sparse matrix is formed using Split-Spectrum Processing, which enhances the signal-to-noise ratio. The Randomized Hough transform is then applied on the sparse matrix elements to detect the hyperbolas that characterize the crack defects.

Keywords Automated inspection · Ultrasonic imagery · Sparse matrix · Defect characterization

T. Merazi Meksen (✉) · B. Boudraa · M. Boudraa
University of Science and Technology H. Boumedienne, BP 32, El Alia, 16111 Bab Ezzouar, Algiers, Algeria
e-mail: t_merazi@yahoo.fr

R. Drai
Center of Welding and Control, Route de Dely Brahim, Cheraga, Algiers, Algeria

1 Introduction

In non-destructive testing of materials, manual ultrasonic systems have been successfully employed for many years using handheld probes, which produce rectified A-Scan signals from the reflected ultrasound. The rectified signals are dynamically viewed by a technician who interprets various components of the displayed A-Scan, including shape, time displacement and amplitude.

When large structures are inspected, the amount of data produced can be extremely large. Automated data acquisition systems have been developed, and various methods such as the neural network, pattern recognition and knowledge-based systems are used to reduce the influence of human factors [1–4]. The appearance of computing systems capable of rapidly processing the recorded signals and creating images has resulted in a steady improvement in the possibilities of non-destructive testing. More than a convivial representation of the results, ultrasonic imagery allows the operations of detection, location and sizing of defects present in the structure to be carried out automatically [5–7]. However, data processing and interpretation of images requires expert knowledge, and the accuracy is largely dependent on the experience of the operator. In light of industrial pressure, the recent trend has been to automate image interpretation processing using software.

Many works have reported on automated interpretation of ultrasonic images. G. Swamy et al. described a method where the crack tip positions are estimated from the local maxima of a correlation function between the filtered image (containing only the discontinuity pixels) and a simulated one (by calculation of the diffracted arcs under the same experimental conditions) [8]. G. Baskaran and K. Balasubramaniam developed an automatic defect detection algorithm to locate crack tips by first separating the echo signal from

superimposed signals and then processing it using a standard valley detection algorithm [9].

M.C. Robini used a method based on the wavelet packet transform [10]. The detection process operates on detailed images obtained from successive wavelet packet decomposition. The flaw information is then extracted using a statistical selection procedure, which is based on the detailed image histograms.

Automated discontinuity detection using neural network-based concepts has also been reported [11–13].

The Hough transform is a classical tool of pattern recognition that has demonstrated good robustness in object detection [14]. It has been used by F.C. Lew [15] to automate the detection of crack defects that are characterized by sets of hyperbolas in TOFD images. The Hough space is computed within a gradient analysis, where relative maxima correspond to the position of the crack top. K. Maalmi proposed the use of an inverse Hough transform, where the voting process is performed in the image space rather than in the parameter space [16]. Here the local peak detection problem is converted to a parameter optimization problem, which is solved using a genetic algorithm.

In an earlier work, we demonstrated that this method can be extended to detect circular defects, such as inclusions [17]. However, we noted that the amount of data necessary for processing is too large, resulting in long processing time.

In addition to processing time and memory consumption (considering all pixels during the processing), the performances of all of the methods cited above are limited by high noise; because the diffracted echo is 20 dB lower than the reflected one, if the instrument sensitivity (gain) is set at a very low level, the TOFD image would display no signal. If the instrument sensitivity is set just above the electronic noise level, the image will display numerous diffracted echoes, which are caused by very small inhomogeneities and do not imply that the structure contains a defect.

In this paper, we illustrate the feasibility of incorporating an algorithm into the software to improve the detection and characterization of a crack without forming an image, instead replacing it with a sparse matrix. In fact, in ultrasonic images, the zone of interest is often very small in comparison with the image dimensions. It is therefore beneficial to use this special matrix type (termed a sparse matrix), where only the non-zero elements are stored, to reduce the amount of stored data. In addition, operations on this type of matrix can take advantage of a priori knowledge of the positions of non-zero elements to accelerate the calculations.

The elements of the sparse matrix form hyperbolas, which are sufficient to characterize the crack defect being detected. Those elements will be selected from the diffracted signals by using the Split-Spectrum Processing method (SSP). Thus, the signal-to-noise ratio is improved, and the position of the echo signal is accurately determined.

In the decision phase, the Randomized Hough Transform (RHT) is applied on the sparse matrix elements to detect hyperbolas. The peak positions of obtained Hough space correspond to the crack tips presented in the structure under control. This paper is organized as follows: Sect. 2 describes classical TOFD image formation, while Sect. 3 contains the description of the measurement conditions. Section 4 describes the Split-Spectrum processing phase and sparse matrix formation. In Sect. 5, the application of the Randomized Hough transform is presented. Sections 6 and 7 highlight the results and conclusions, respectively.

2 Image Formation

When ultrasound is incident to a linear discontinuity, a diffracted energy is emitted over a wide angular range and is assumed to originate at the tips of the discontinuity. This makes the ultrasonic method based on diffracted waves ideal for detecting flat defects such as cracks. This method, termed TOFD (Time-Of-Flight Diffraction), is also slightly influenced by an unfavorable orientation of the discontinuity.

Usually, a TOFD image is formed using a symmetrical and separate transmitter-receiver shear wave pair of transducers with an angle of incidence of 45°, 60° or 75°. This tandem is moved automatically step-by-step in a straight line, and the diffracted signals are recorded and displayed on a grey scale. Samples of every reached signal constitute a row of the TOFD image, and the delay time is linked to the depth of the defect in the structure. Figure 1 shows an example where echoes relative to surface and back wall echoes have been filtered out.

When the present defect is a crack, it will appear on the image as a set of hyperbolas along the main axis. The multiple diffraction arcs are due to the type of the pulse transmitted and received by the transducers, and the summit points are related to the tip of cracks.

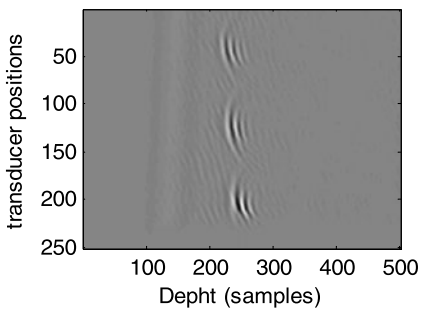

Fig. 1 TOFD image containing three defects. 500 samples of each reached signal are represented for 250 positions of the transducers

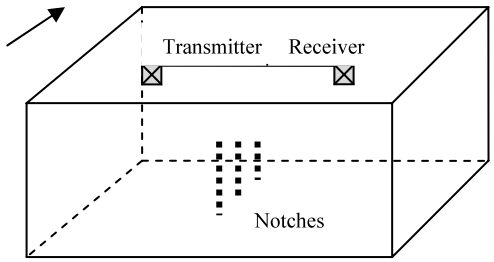

Fig. 2 Test block with three artificial defects

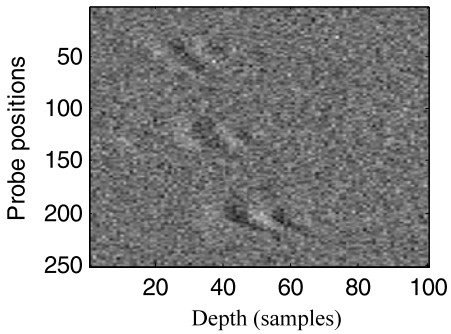

Fig. 3 Zone of interest of the TOFD image in Fig. 1

3 Measurements

In this work, a test block containing three artificial defects was used. The defects in the form of notches were located at different depths. Data acquisition was made following the basic principle of the TOFD technique. The tandem of the transducers (one serving as a transmitter and the other as a receiver) was moved step-by-step along a straight line and using a step resolution of 1 mm. In Fig. 2, the arrow indicates the scanning direction followed by the transducer pair.

To test this method under a condition of a low SNR ratio, a simulated Gaussian noise signal was superimposed on each reached signal. The classical TOFD image that results in this situation is shown in Fig. 3. Detecting defects on such a noisy image can be difficult.

In order to show closely the defect region, the zone of interest of the TOFD image above was formed using only the one hundred samples from each obtained signal, containing the interesting samples.

4 Split-Spectrum Processing Phase

4.1 Principle of the SSP

Split-Spectrum Processing is a practical implementation of the frequency diversity concept. It has been successfully used for flaw detection and noise suppression in NDT applications [18]. In SSP, a diverse frequency ensemble is created from the wideband input signal by employing a set of parallel band-pass filters with different center frequencies. The received signal spectrum is partitioned into different frequency band-pass filters to obtain a set of narrowband signals $x_1(n), x_2(n), \ldots, x_N(n)$. The maximum amplitude of each narrowband signal is then scaled to unity by the factors w_i, and the N signals $w_1x_1(n), w_2x_2(n), \ldots, w_Nx_N(n)$ are subsequently processed using various linear and nonlinear operations to obtain the output time signal $y(n)$.

The spectrum of the received echo is obtained by performing a Discrete Fast Fourier Transform. Zero padding of the signal in the time domain is used before the SSP to increase the frequency resolution.

In this work, Gaussian filter function has been used to split the spectrum and the output time signal $y(n)$ is calculated within the minimization method.

4.2 Application of the SSP Minimization Method

Gaussian band-pass filters with different mean (f_1, $f_2, \ldots, f_N$) and constant variance of $\sim f/2$ are used to split the spectrum into several overlapping bands so that none of the frequency components of the original signals are lost in the processing.

It is well known that the optimum frequency separation of the filters is:

$$\Delta f = 1/T \tag{1}$$

where T is the total time duration of the ultrasonic signal.

Theoretically, a time-limited signal produces an infinite bandwidth. However, because of the frequency response of the transducer, the only usable spectrum is limited to a frequency band B Hz. Thus, the number of uncorrelated frequency bands N of bandwidth B is:

$$\check{N} = B/\Delta f = B.T \tag{2}$$

Therefore, the actual number of filters that could be used is:

$$N = \check{N} + 1 \tag{3}$$

Different split spectra were then produced by passing through overlapping Gaussian filters with different center frequencies. The time domain signal $x_i(n)$ of each individual frequency bands can be found by computing an Inverse Fast Fourier Transform. The maximum amplitude of each narrowband signal is then scaled to unity by the factors w_i. Thus, $|w_ix_i(n)|$ represents the magnitude of the ith narrowband filter output and the output $y(n)$ of the absolute minimization algorithm for each time instant n is expressed as:

$$y(n) = \min(|w_ix_i(n)|, \ldots, |w_Nx_N(n)|) \tag{4}$$

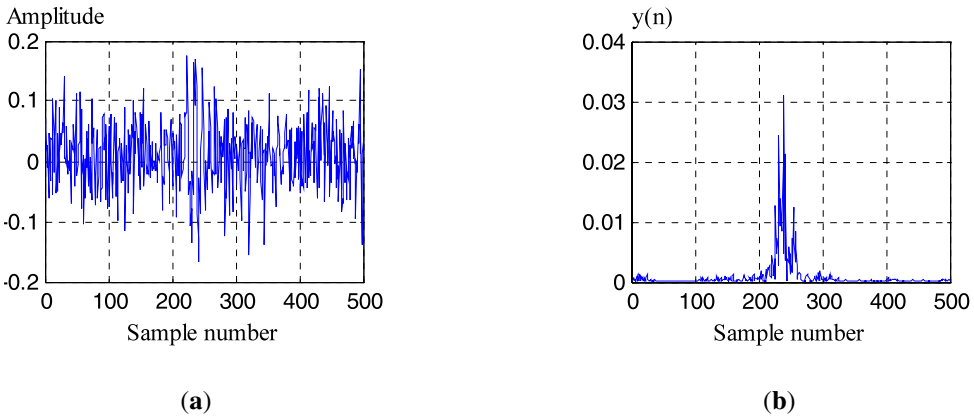

Fig. 4 A typical processed result: (**a**) example of an A-scan reached signal with superimposed noise; (**b**) the SSP-processed result

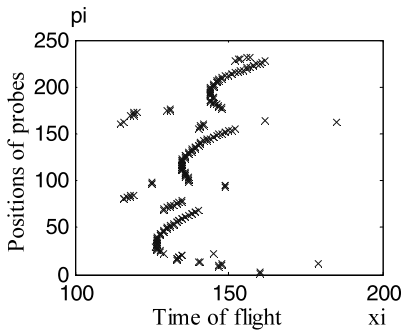

Fig. 5 Sparse matrix obtained under the same conditions as the TOFD image in Fig. 1

Figure 4(b) shows the processed result of the noisy signal from Fig. 4(a).

As shown in Fig. 4 (b), the result of the SSP processing produces a peak that can be used to echo location within a unique sample. Thus, in the data storage phase, if only the probe position (p_i) and the horizontal peak coordinate (x_i) are considered, then at the end of the scanning, a sparse matrix will be built.

Figure 5 demonstrates the result obtained when this method is applied using signals that has constituted the TOFD image on Fig. 3. A substantial reduction in required memory and time is achieved if only the coordinates of those points are stored. In fact, from the 250×500 pixels of the TOFD image, calculations need only be done on 180 resulting points.

5 The Hough Transform

5.1 Principle of the Hough Transform

The Hough transform was initially developed for the detection of points aligned on a straight line. More generally, it can detect more complex shapes as long as a mathematical model can be defined for these shapes. The Hough transform considers all of the possible positions and orientations of the shape (for example, all of the possible values for the parameters a and b of a straight line defined by the equation $y = ax + b$ in the x–y plane). Next, for each position and orientation (defined by a particular value of the parameters a and b), the number of contributing points in the source image is counted and stored in a ceil of an accumulator called Hough space. In the decision step, a threshold for the number of contributing points is defined, and all of the straight lines defined by the parameters (a, b) such that the number of contributing points in the source image is greater than the threshold are determined.

5.2 Randomized Hough Transform

In the classical approach, one pixel is mapped into all the points on a line passing by a diverging mapping mechanism. The Randomized Hough transform, established by L. Xu is an approach which replaces this mechanism with a converging mapping mechanism such that two pixels are picked to jointly determine a line. Thus, different points in the same line will hit the same point in the Hough space without creating a great number of false accumulations. This enables several joint improvements, such as random sampling in place of point scanning, a small accumulator size and an adaptive detection in place of enumerating all the points [19].

5.3 Detection of Hyperbolas

An hyperbolas is defined as a unit of points checking the equation:

$$(x - x_0)^2/a^2 - (y - y_0)^2/b^2 = 1 \tag{5}$$

Parameters a and b depend of the hyperbola eccentricity, x_0 and y_0 are the summit coordinates.

The algorithm that describes the processing follows the steps bellow:

Algorithm

– An accumulator $A(x, y)$ is set to zero.
  For a fixed number of iterations:
  {
  – Three elements are randomly selected
  – The coordinates (x_0, y_0) of the summit of the hyperbola containing those 3 elements are calculated
  – The corresponding ceil is incremented:

$$A(x_0, y_0) = A(x_0, y_0) + 1 \tag{6}$$

  }

In the decision phase, relative maximums of A correspond to the positions of the summits.

6 Results and Discussion

Applying the algorithm described above to the elements of the sparse matrix stored, the Hough space was obtained (Fig. 6), showing three peaks corresponding to the three artificial cracks. Their coordinates indicate the positions of their bottoms.

This algorithm was also tested for the case of a real defect initially detected by the classical TOFD technique. The tandem of probes was moved step-by-step perpendicular to a generator retaining ring, and the resulting TOFD image (Fig. 7) illustrates the set of parabolas corresponding to the crack. Horizontal lines correspond to back wall echoes.

Figure 8 represents the sparse matrix obtained in this case when processing the region defined by the square on the TOFD image above. The circular red point indicates the summit of the crack.

In the case of a crack entirely included in the structure, both the top and bottom tips involve peaks. As echoes diffracted from the upper and lower extremities are expected to be 180° out of phase, correct exploitation of this phase information helps in its interpretation. In this case, the length of the crack is estimated directly from the distance between the peaks, and the orientation of the crack is thus determined.

This method is limited in the case of cracks close to the surface, where a lateral wave obscures the tip diffracted signal.

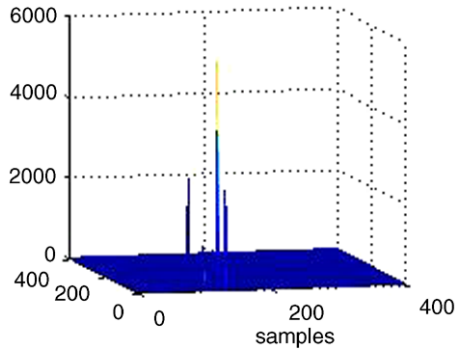

Fig. 6 Hough space of the sparse matrix represented in Fig. 5. The three peaks correspond to the three cracks detected

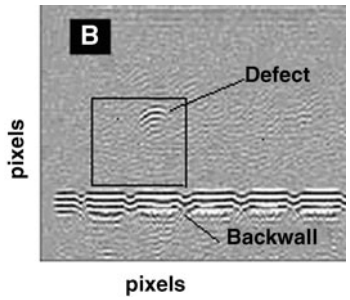

Fig. 7 TOFD image of a crack on a generator retaining ring

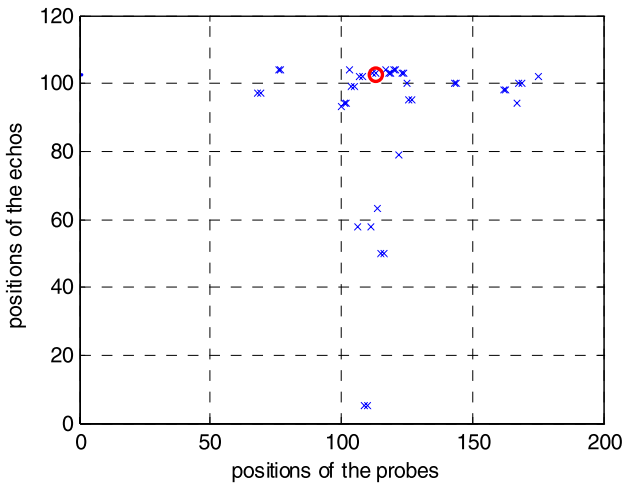

Fig. 8 Sparse matrix obtained by scanning a generator retaining ring

7 Conclusion

In this paper, we have demonstrated the feasibility of an automated ultrasonic method that allows the detection and characterization of cracks presented in a structure. This method reduces human intervention, the quantity of data stored and the necessary processing time. It avoids the TOFD image formation usually exploited in NDT techniques, instead replacing it with a sparse matrix. In the de-

cision phase, the use of the Randomized Hough Transform allows automatic detection even if the curve is occluded, as isolated points are very unlikely to contribute to a peak in Hough space. Incorporating this method into the software used in automatic systems will help in decision making. In the case of small cracks, echoes due to the two tips may overlap. Future work consists of performing the SSP method to distinguish between two close signals.

References

1. Shuxiang, J.: Development of an automated ultrasonic testing system. In: 3rd International Conference on Experimental Mechanics, Singapore, 2004. SPIE Proceeding, vol. 5852. SPIE, Bellingham (2004)
2. Bavendiek, K., Herold, F.: Defect recognition in industrial applications. In: Proceeding of International Workshop of Imaging in *NDE*, INDE, Hamburg, Germany (2007)
3. Baker, A.R.: The classification of defects form ultrasonic data using neural networks: the Hopfield method. NDT Int. **22**(1), 97–105 (1989)
4. Webber, S.A.: Five years of testing using the semi-automated ultrasonic time of flight diffraction system. In: 10th APCND, Austria (2001)
5. Miller, M.: Development of automated real-time data acquisition system for robotic weld quality monitoring. Mechatronics **12**(9–20), 1259–1269 (2002)
6. Passi, G.S.: Reducing the influence of human factors on the reliability of manual ultrasonic weld in inspection. Insight **37**(10), 788–791 (1995)
7. Martin, J., Gonzalez, R.: ULTRASCOPE TOFD: un sistema compacto para la captura y procesamiento de imagine TOFD. In: IV Conferencia Panamericana, de END, Buenos Aires (Oct. 2007)
8. Swamy, G., Baskaran, G.: A point source correlation technique for automatic discontinuity identification and sizing using time of flight diffraction. Mater. Eval. **63**(4), 425–429 (2005)
9. Baskaran, G., Balasubramanian, K.: Ultrasonic TOFD flaw detection sizing and imaging in thin plates using embedded signal identification technique (ESIT). Insight **46**(9), 537–542 (2004)
10. Robini, N.C., Magenin, I.E.: Two-dimensional ultrasonic flaw detection based on the wavelet packet transform. IEEE Trans. Ultrason. Ferroelectr. Freq. Control. **44**(6), 1382–1394 (1997)
11. Lawson, S.W., Parker, G.A.: Automatic Detection of Defects in Industrial Ultrasound Images Using Neural Networks. Proceeding of SPIE, vol. 2786, pp. 37–47. SPIE, Bellingham (1996)
12. Shekhar, C., Shitole, N.: Combining fuzzy logic and neural networks in classification of weld defects using ultrasonic time of flight diffraction. In: 45th Annual British Conference on NDT, NDT 2006, Stratford-upon-Avon, UK (September 2006)
13. da Silva, I.C., Siqueira, M.H.S.: Automatic inspection using the TOFD technique and neural networks. In: 8th European Conference in Non Destructive Testing, ECNDT, Barcelona (2002)
14. Maitre, H.: Un panorama de la Transformée de Hough. Rev. Trait. Signal. **2**(4), 305–317 (1985)
15. Von Lew Yan, L.F.C.: Gradient based hough transform for the detection and characterization of defect during non destructive inspection. In: Proceeding of Symposium on Electronic Imaging Science and Technology, vol. 3029, pp. 140–141, California (1997)
16. Maalmi, K.: Crack defect detection and localization using genetic-based inversion voting hough transform. In: 16th International Conference in Pattern Recognition ICPR'02, vol. 3, Quebec City, (11–15 Aug. 2002)
17. Merazi Meksen, T., Drai, R.: Pattern recognition in ulrasonic imagery using the hough transform. In: Proceeding of World Conference of Ultrasonics WCU2003, Paris (Sept. 2003)
18. Yau, K.K.: Split spectrum processing for non destructive testing, NDTnet, No08. http//%20www.ndt.net/article/splitspec (Aug. 1999)
19. Xu, L., Oja, E.: Randomized hough transform (RHT) basic mechanisms. Algorithms Comput. Complex., Image Underst. **57**(2), 131–154 (1993)